VOL 2 NO 7: JULY, 2025
AN OPEN ACCESS PEER-REVIEWED JOURNAL
Frontline Professionals Journal 2(7), 28-39, EISSN *1596-0501*

Original Research

EFFECT OF DEPOSITION TIME OF POTASSIUM PERMANGANATE NANO THIN FILMS ON EDDY CURRENT REDUCTION IN TRANSFORMER CORES

Authors: Francis, Victor Akoma[1]; Nwabuzor, Peter Onyelukachukwu[1]; Sofolabo, Adekunle Oyemade[2]

[1]Department of Physics with Electronics Technology, School of Science Laboratory Technology, University of Port Harcourt, P.M.B 5323 Choba, Port Harcourt, Nigeria
[2]Department of Physics, University of Port Harcourt, P.M.B 5323 Choba, Port Harcourt, Nigeria

Corresponding Author Email: victor.francis@uniport.edu.ng;

Authors' contributions
This study was a collaborative effort among all authors. Each author reviewed and approved the final version of the manuscript for publication.
Article Information
EISSN 1596-0501
Website: https://frontlineprofessionalsjournal.info
Email: frontlineprofessionalsjournal@gmail.com

CITATION: Francis, Victor Akoma, Nwabuzor, Peter Onyelukachukwu and Sofolabo, Adekunle Oyemade (2025). Effect of deposition time of potassium permanganate nano-thin films on eddy current reduction in transformer cores. *Frontline Professionals Journal* 2(7), 28-39

ABSTRACT
This study looks at using potassium permanganate ($KMnO_4$) thin films, made through electrochemical methods, as a substitute for laminating transformer cores on soft iron materials. The study aimed to describe the electrical and crystal properties of $KMnO_4$ films after they were deposited for different lengths of time (from 5 to 20 minutes) and to compare the results with a control made of silicon iron steel. Four samples of $KMnO_4$ (X_1,X_2,X_3 & X_4) were deposited at different intervals (5,10,15 & 20) minutes respectively. Characterization of the deposited films with X-ray diffraction (XRD) validated the crystalline structure of $KMnO_4$ nanoparticles, demonstrating consistent peak positions at 2θ angles of 45.2° and 65.4° across the various deposition times, with d-spacing values of 1.96 Å and 1.42 Å, respectively. The Result showed that sample X_4 (the Sample with the highest deposition time of 20minutes) has the strongest intensity count of 26.61, indicating that longer deposition time increases the intensity, which in turn enhances crystallinity, alignment, and stable crystal size within the thin film. Similarly, electrical investigation showed that increasing the deposition time of $KMnO_4$ films improves resistivity and reduces conductivity, resulting in a reduction in eddy current losses and increased energy efficiency.

Keywords: Potassium Permanganate ($KMnO_4$), Deposition time, Eddy Current loss, Transformer core

1.0 INTRODUCTION

Transformers are essential components of modern power systems; their primary function is to adjust voltage levels, making them essential to the generation, transmission, and distribution of electrical power (Theraja, 2005). Arritt and Dugan (2008) disclosed that transformers provide electrical isolation between circuits, safeguarding equipment and ensuring safety by preventing direct connections between high and low voltage systems. Transformers consist of significant parts (components) including the core, windings, insulation, and tank. The core, typically made of laminated silicon steel, minimizes losses resulting from eddy currents and hysteresis (Fernández et al., 2013). Windings are coils of

wire wound around the core, it is where the energy transfer from the primary to the secondary circuits occurs. Insulation prevents electrical short circuits, and the insulation and heat dissipation are provided by the tank, typically filled with insulating oil (Ye et al., 2020). The performance, efficiency, and reliability of transformers largely depend on several types of losses that take place in them. These losses are caused by several sources such as the transformer's windings, magnetic core, tanks, as well as other metal components of the transformer. (Olivares-Galván et al., 2009) classified the transformer loss problem into three categories at large: (a) high-current bushing tank losses, (b) core joint transformer core losses, and (c) stray transformer tank losses. Among these losses, eddy currents are a specific problem. Eddy currents are circular flows of electric current that are generated inside the core material of a transformer by varying magnetic fields. These currents generate heat within the core, leading to loss of energy, elevated operating temperature, and reduced total efficiency. Researchers to date have had somewhat varying methods of reducing such losses and improving transformer efficiency, some of which are presented here with their objectives and achievements.

A study presented in Frljić, Trkulja, & Žiger, (2021), whose aim was to improve the way that the eddy current losses were calculated in the laminated open-type transformer core configurations using a certain numerical format. They sought to increase the precision and speed of computing eddy current losses, which are very important in the design of transformers. The authors proposed a method for the A, T − A expression (with the electric vector potential T) rather than A,V − A formulation. This method provides better mixing of the core but previously suffered from poor simulation convergence due to a high number of degrees of freedom. By eliminating redundant degrees of freedom, their method significantly improved convergence rates, achieving at least twice the efficiency compared to the traditional formulation. The results were validated by comparing them with simulations using the A, V−A formulation. This study is relevant to current research on transformer cores, particularly in optimizing core designs to reduce eddy current losses effectively. Similarly, Yu et al., (2020) investigated the impact of different iron core materials on the performance and efficiency of a single-phase transformer during out-of-phase synchronization in a microgrid. Their study aimed to address the limitations of previous analyses, which often neglected core saturation effects. By employing finite element methods, the researchers explored how variations in core material and the BH curve influence the electromagnetic behavior of saturated transformers. They found that the impact current, core permeability, and magnetic field strength are closely linked to both the type of core material used and the position of the switch. Additionally, the study provided insights into the harmonic components of impulse current from the power grid and generator. These results highlight the critical role of core material selection in enhancing transformer performance and managing synchronization issues in power systems.

The study by Kaur and Kaur (2019) examined the effect of core materials on the performance of single-phase transformers using Finite Element Method (FEM) analysis. They aimed to evaluate how different core materials—CRGO silicon steel, Amorphous steel, and Finemet—affect transformer performance, with a focus on reducing operational losses. They employed a 3-D FEM analysis to compare these materials and their impact on transformer efficiency. The results highlighted the comparative effectiveness of each core material in minimizing losses, providing valuable insights into the optimal selection of materials for transformer design. The study's findings are relevant to current research on improving transformer efficiency through material selection, as they contribute to understanding how different materials influence transformer performance and loss reduction. In 2012, Wasan, et al., used two different sol-gel processes to produce ZnO thin films: dip coating and spin coating. The films were deposited onto a glass substrate at ambient temperature using a sol-gel comprised of zinc acetate dehydrate, monoethanolamine, isopropanol, and deionized water. The films were then warmed at 225°C for 15 minutes. The crystallographic structures of ZnO films were investigated using X-ray diffraction (XRD); the results show that the good film was prepared using the dip coating technique, was polycrystalline, and had a high c-orientation along the (002) plane; the lattice constant ratio (c/a) was calculated at (002) and was approximately 1.56. The structure of thin films created using the spin coating process was amorphous, with low intensity and wide peaks. Norhidayah et al. (2015) prepared ZnO thin films by sol–gel spin coating technique. The effects of solution ageing times which varies at 2h 15 min, 3h 30 min and 24h were investigated. The structural and morphological were studied using an x-ray diffractometer and atomic force microscope respectively. Based on the XRD measurement, it was revealed that ZnO films were polycrystalline with hexagonal wurtzite structure. The crystallite size is in the range of 34.4 ~ 28 nm which decreased with ageing time increment. On the other hand, the AFM analysis revealed that the surface roughness of the

films increased due to the increment of ageing times. From the reviewed literatures it can be clearly seen that no researcher has considered the effects of deposition time and the use of Potassium Permanganate Nano Thin films as alternative material in lamination of transformer core for reduction of eddy current. Nanotechnology offers a promising alternative for addressing these challenges. By leveraging materials at the nanoscale, researchers can develop advanced coatings with superior insulating properties to minimize eddy currents. This study focuses on synthesizing potassium permanganate thin films using electrochemical deposition techniques and applying them to transformer cores. The aim is to investigate the effect of deposition time in the evaluation of the effectiveness of these coatings in reducing eddy current losses while enhancing transformer performance.

2.0 METHODOLOGY 2.1 Materials

Some of the materials used to carry out this research are Digital Multimeter, DC Power Supply, Saturated Calomel Electrode, Thermometer, Ultrasonic Bath, Potassium Permanganate ($KMnO_4$), X-ray Diffractometer (XRD) etc.

2.2 Methods 2.3 Research Design

The research design involved experimental synthesis of thin films followed by analytical evaluation that covered the following: Synthesis of potassium permanganate thin films via electrochemical deposition, Application of these films onto iron cores, Characterization of film properties using XRD, Evaluation of their impact on reducing eddy current losses.

2.4 Experimental Procedure

The following experimental processes were followed: Selection of Materials, Procurement of Iron Cores, Core Preparation/ Substrate Treatment, Preparation of Thin Film Solutions, Electrochemical Deposition Apparatus Setup, Post-Coating Processing, Characterization of Thin Films (XRD), Conductivity Test Apparatus Setup

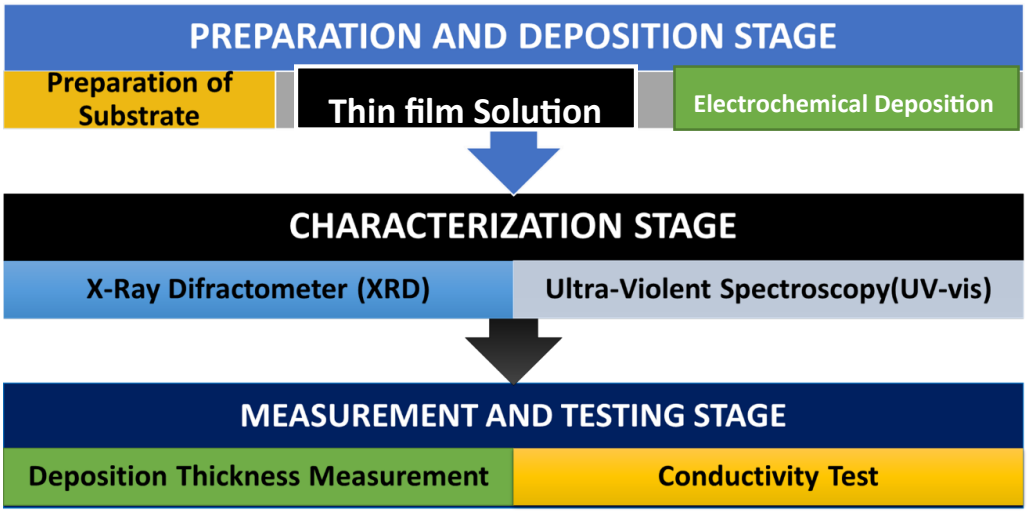

Figure 1: Experimental Procedures Flow Chart

Potassium permanganate was chosen for its high resistivity and compatibility with iron cores due to its dielectric properties. Iron cores were extracted from a dismantled single phase transformer. The rust and impurities were removed using sandpaper and the cores were cleaned with distilled water, acetone solution, and ultrasonic baths before they were dried in an oven to get it ready for the coating. 1.5g of $KMnO_4$ was dissolved in 100ml of distilled water, it was stirred until completely dissolved. Once dissolved it was ready for use and was poured into the electro-chemical deposition beaker (bath), where the substrate (transformer core) was deposited w ith the $KMnO_4$ at different time frames (5 minutes, 10 minutes, 15 minutes and 20 minutes). The process was followed through for all substrate samples that need to be deposited into the five iron core and glass surfaces. Thin films were deposited electrochemically onto iron cores using a DC power supply set at 10V. Deposition times ranged from 5–20 minutes and longer deposition times produced thicker

coatings. After applying the thin film, the coated iron cores undergo post-coating processing. This includes curing, which may involve heating the cores to ensure that the thin film sticks properly and achieves the desired properties.

Plate 1: Experimental setup for the electrolytic deposition process

2.5 Characterization of Thin Films: The characterization of thin films is performed to assess their properties and effectiveness. Techniques such as X-ray diffraction (XRD) is used to analyze the morphology, thickness, and structural properties of the thin films. The characterization starts from when the deposited substrate (soft iron core and FTO glass) is feed into the XRD machine in order to get and analyze all properties of the deposited thin films. This step is critical for evaluating the performance of the thin films in reducing eddy currents and ensuring that they meet the desired specifications. For example using Bragg's law, the interplanar spacing of the deposited thin film can be deduced from the XRD result as shown in equation 3.4 and 3.5 below

$n\lambda = 2d\sin\theta$ 1

Where n is the order of reflection (n = 1), λ is the X-ray wavelength (e.g., 1.5406 Å for Cu Kα radiation), θ is the angle of diffraction and d is the interplanar spacing. From equation 1, the interplanar spacing is deduced as shown in equation 2.

$$d = \frac{n\lambda}{2\sin\theta} \quad 2$$

Similarly the crystal size (D) (nm) can be estimated using the Scherrer equation as shown

$$D = \frac{K\lambda}{\beta\cos(\theta)} \quad 3$$

Where; K is the shape factor (typically 0.9), and β represents peak broadening due to crystal size effects = 0.

Plate 2: Picture of XRD machine used for the Characterization

3.0 RESULTS

Figure 2 and Table 1 present an XRD result that reflect the crystallographic analysis of potassium permanganate ($KMnO_4$) nanoparticles used in the thin-film synthesis at 5 minutes deposition. The X-ray diffraction (XRD) result showed two notable peaks at 2θ angles degrees of 45.2˚ and 65.4°, with respective intensity counts of 25.4 and 4.59 respectively. Using Bragg's Law interplanar spacing (d-spacing) for the peak at the respective 2θ degrees were 1.96A˚ and 1.42A˚ and the crystal sizes were determine using Scherrer equation to be 4.65nm and 5.5nm respectively.

The corresponding results for the four (4) various time of deposition of Potassium Permanganate ($KMnO_4$) are shown in the figures and tables below:

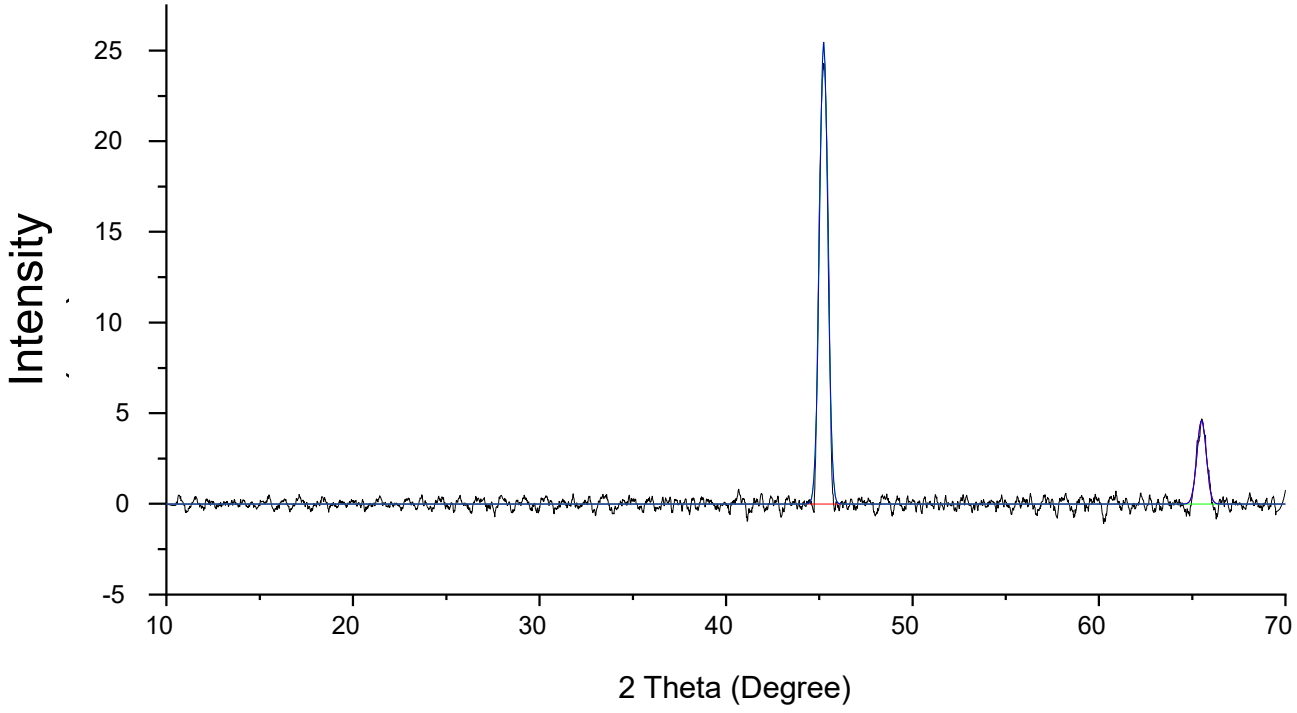

Figure 2: XRD pattern of $KMnO_4$ deposited for 5 minutes

Table 1: Deposition Analysis of Potassium Permanganate ($KMnO_4$) at 5 Minutes

Hkl	**2θ (degrees)**	**Intensity (counts)**	**Wavelength (λ) (nm)**	**FWHM**	**Interplanar Spacing (d) (Å)**	**Crystal Size (nm)**
(101)	45.22	25.40	0.154	0.35	1.96	4.65
(210)	65.4	4.59	0.154	0.4	1.42	5.5

Figure 3 and Table 2 below present an XRD result that reflect the crystallographic analysis of potassium permanganate ($KMnO_4$) nanoparticles used in the thin-film synthesis at 10 minutes deposition. The X-ray diffraction (XRD) result showed two notable peaks at 2θ angles degrees of 45.2˚ and 65.4°, with respective intensity counts of 14.15 and 3.04 respectively as shown below.

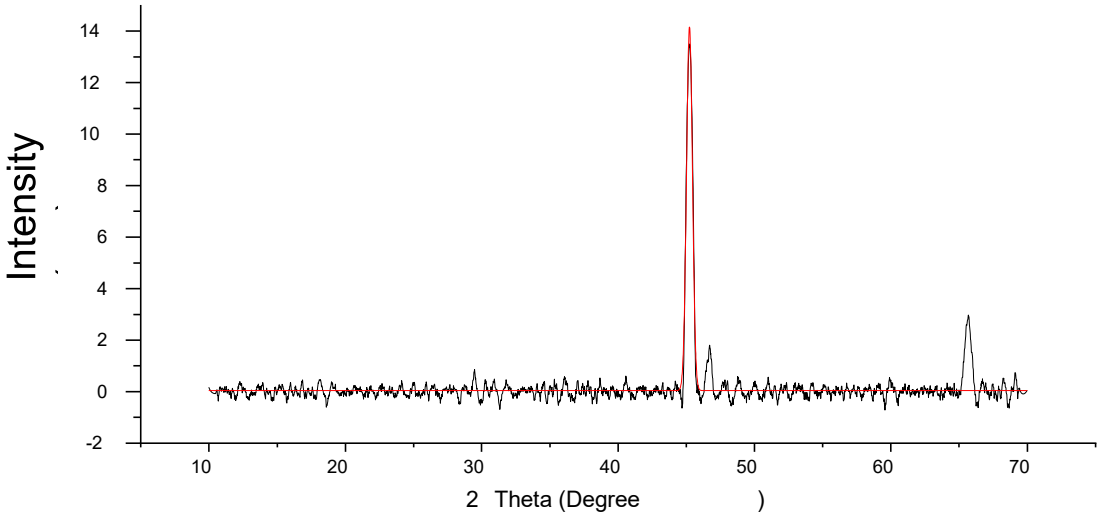

Figure 3: XRD pattern of $KMnO_4$ deposited for 10 minutes

Table 2: Deposition Analysis of Potassium Permanganate ($KMnO_4$) at 10 Minutes

Hkl	2θ (degrees)	Intensity (counts)	Wavelength (λ) (nm)	FWHM	Interplanar Spacing (d) (Å)	Crystal Size (nm)
(101)	45.22	14.15	0.154	0.45	1.96	4.65
(210)	65.4	3.04	0.154	0.42	1.42	5.5

In Figure 4 and Table 3 showed the XRD result that reflect the crystallographic analysis of potassium permanganate ($KMnO_4$) nanoparticles used in the thin-film synthesis at 15 minutes deposition time frame is presented. The result also showed two notable peaks at 2θ angles degrees of 45.2˚ and 65.4°, with respective intensity counts of 26.61 and 12.69 respectively.

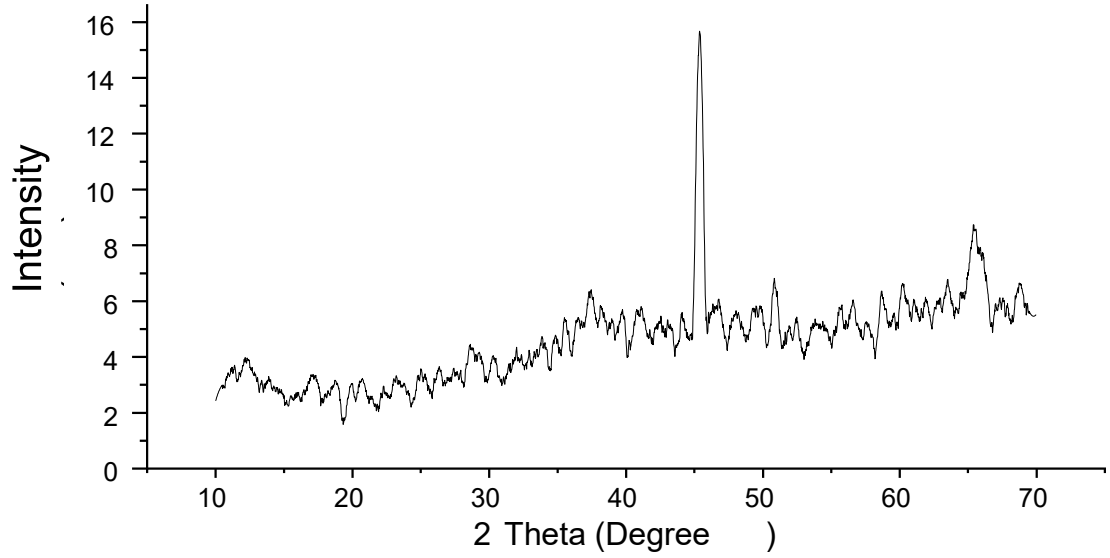

Figure 4: XRD pattern of $KMnO_4$ deposited for 15 minutes

Table 3: Deposition Analysis of Potassium Permanganate (KMnO) at 15 Minutes

Hkl	2θ (degrees)	Intensity (counts)	Wavelength (λ) (nm)	FWHM	Interplanar Spacing (d) (Å)	Crystal Size (nm)
(101)	45.22	15.67	0.154	0.41	1.96	4.65
(210)	65.4	8.70	0.154	0.43	1.42	5.5

Similarly Figure 5 and Table 4 shows the XRD result that reflect the crystallographic analysis of potassium permanganate ($KMnO_4$) nanoparticles used in the thin-film synthesis at 20 minutes deposition. The result followed a consistent pattern showing two notable peaks at 2θ angles degrees of 45.2˚ and 65.4°, and an intensity counts of 15.67 and 8.7 respectively as shown below.

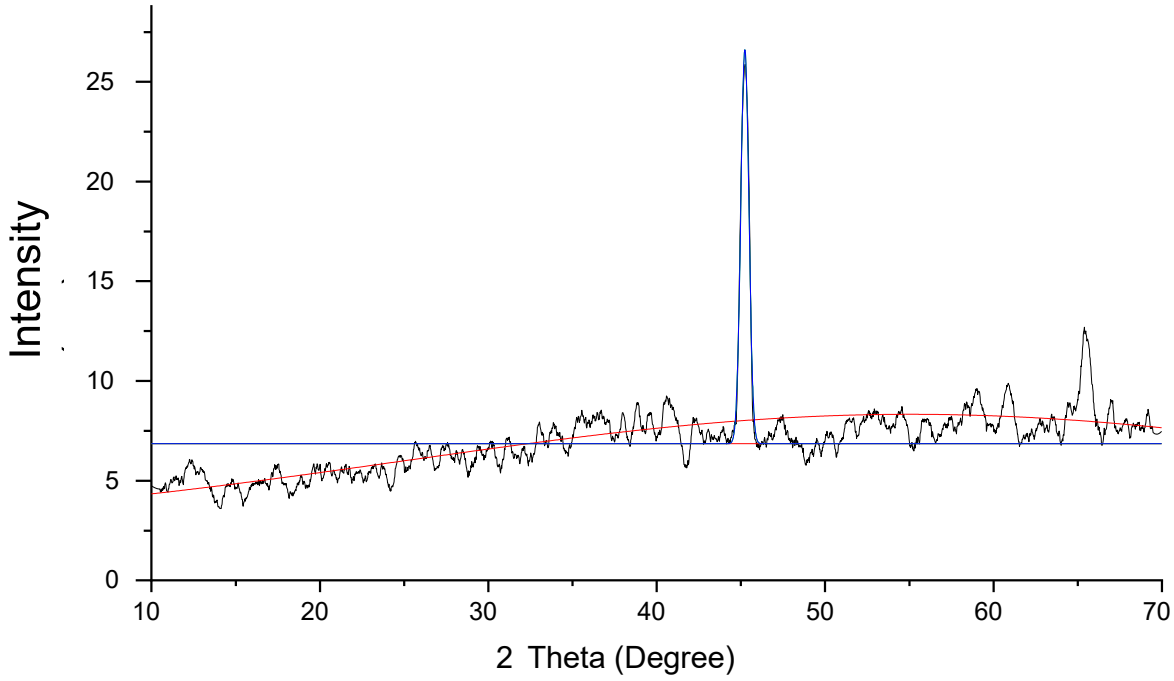

Figure 5 XRD pattern of $KMnO_4$ deposited for 20 minutes

Table 4: Deposition Analysis of Potassium Permanganate ($KMnO_4$) at 20 Minutes

Hkl	2θ (degrees)	Intensity (counts)	Wavelength (λ) (nm)	FWHM	Interplanar Spacing (d) (Å)	Crystal Size (nm)
(101)	45.22	26.61	0.154	0.42	1.96	4.65
(210)	65.4	12.69	0.154	0.44	1.42	5.5

Figure 6 and Table 5 is used to show the XRD result that reflect the crystallographic analysis of Silicon Iron Steel which serves as control element as it is currently used to laminate transformer cores found in the market. The result for the XRD followed a consistent pattern showing two notable peaks at 2θ angles degrees of 45.2˚ and 65.4°, and an intensity counts

of 28.43 and 40.06 respectively. As shown in Figure 6 all various core lamination samples are in a consistent pattern showing two notable peaks at 2θ angles degrees of 45.2˚ and 65.4° at different intensities which shows the closeness of all core samples to each other and their crystalline nature varying at different intensities.

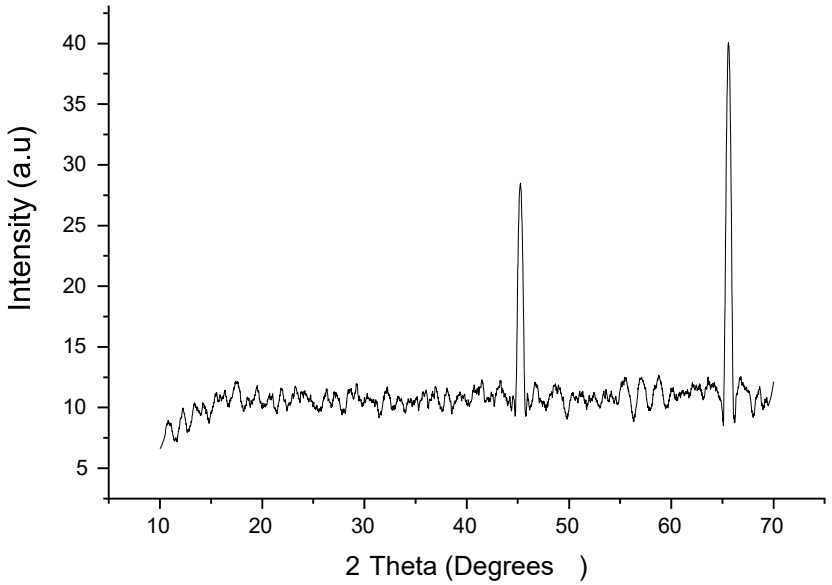

Figure 6 XRD pattern of control element

Table 5: Analysis of Silicon Iron Steel used as the control lamination

Hkl	2θ (degrees)	Intensity (counts)	Wavelength (λ) (nm)	FWHM	Interplanar Spacing (d) (Å)	Crystal Size (nm)
(101)	45.22	28.43	0.154	0.40	1.96	4.65
(210)	65.4	40.06	0.154	0.44	1.42	5.5

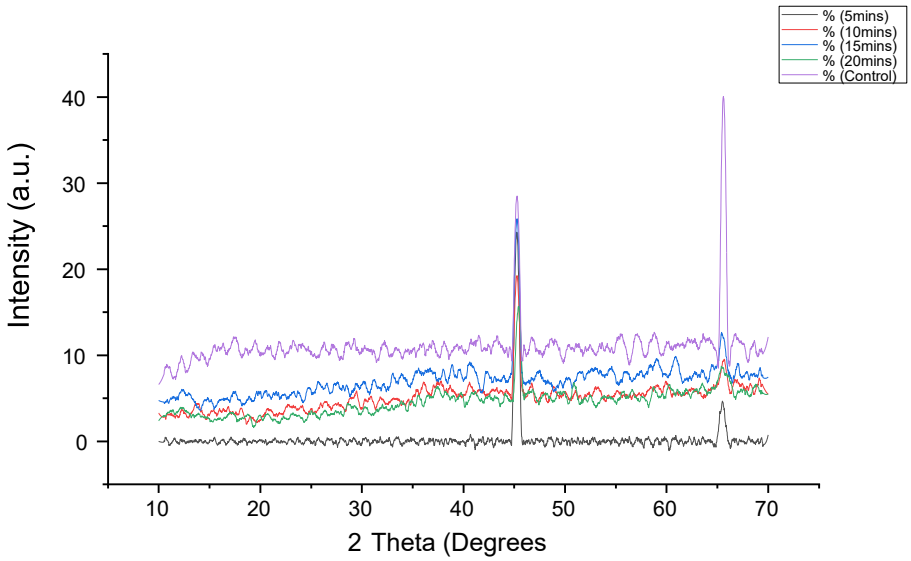

Figure 7: XRD Result Analysis of all compositions

Electrical Investigation of deposited soft iron core (Eddy current): Results from Table 6, provided insights into the relationship between thin film deposition time and electrical properties, specifically resistivity and conductivity, which directly impact eddy current losses in transformer cores. The core sample with the highest resistivity, Sample X4 (deposited for 20 minutes), exhibited a resistivity of 41.04 Ohms/meter and a corresponding low conductivity of 0.0243 Siemens. This high resistivity suggests greater resistance to the flow of eddy currents within the transformer core, which could reduce eddy current losses by limiting unwanted circular currents that lead to energy dissipation as heat. The control sample XE, which was not subjected to any deposition, displayed the lowest resistivity (37.24 Ohms/meter) and highest conductivity (0.0268 Siemens), indicating it would likely experience the greatest eddy current losses due to less resistance to current flow.

Table 6: Conductivity Test Results

CORE SAMPLE	Voltage (V)	Current (mA)	Resistance (Ω)	Resistivity (Ω-m)	Conductivity (S)
X_E	9.8	1.0	9.8	37.24	0.0268
X_4	9.8	0.9	10.8	41.04	0.0243
X_3	9.7	0.9	10.7	40.66	0.0245
X_2	9.3	0.9	10.3	39.14	0.0255
X_1	9.2	0.9	10.2	38.81	0.0257

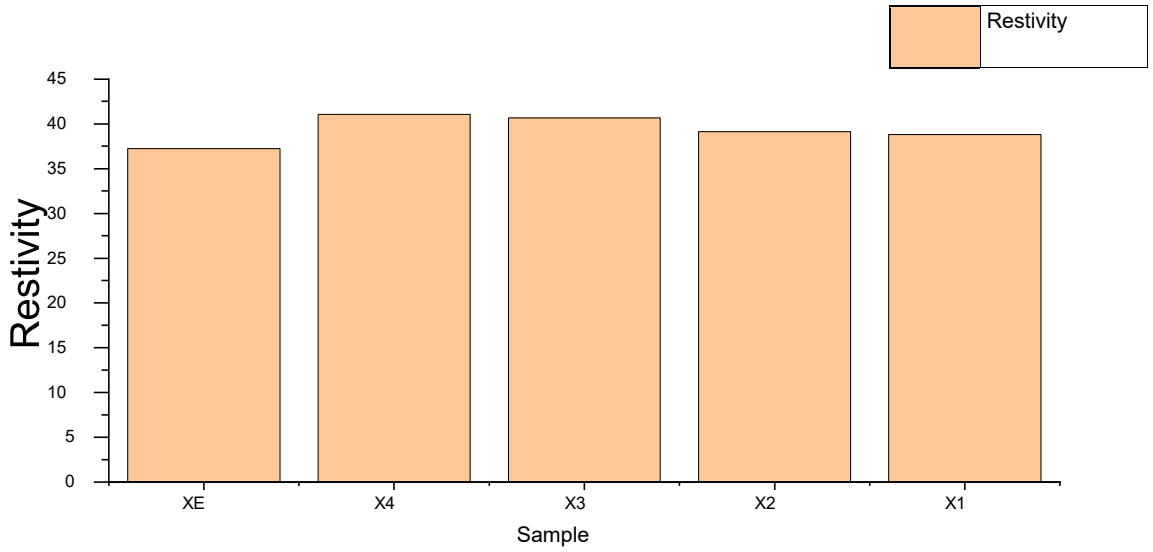

Figure 8. Bar Chart of Sample vs Resistivity

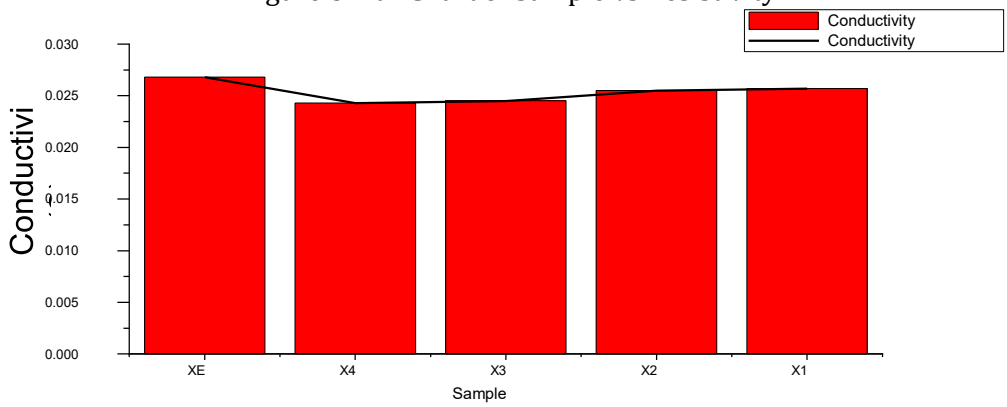

Figure 9. Bar Chart of Sample vs Conductivity

4.0 DISCUSSION

From the result presented in Table 1 XRD examination of $KMnO_4$ nanoparticles deposited for 5 minutes showed two different peaks at 2θ angles of 45.2° and 65.4°. The intensity counts for these peaks were 25.4 and 4.59, respectively. The presence of these peaks shows that the nanoparticles are crystalline, which corresponds to the expected diffraction pattern for $KMnO_4$ based thin films as reported by the findings of (Kate, 2022). The computed d-spacing values for the two peaks at 2θ = 45.2° and 65.4° are 1.96Å and 1.42Å, respectively. These numbers represent the distance between atomic planes in the KMnO4 nanoparticles' crystalline structure which collaborate the discovery of Cullity & Smoluchowski (2014)(Ho et al., 2003). Crystal diameters for peaks at 2θ = 45.2° and 65.4° were determined to be 4.65 nm and 5.5 nm, respectively. The fluctuation in crystallite size can be related to the deposition duration and the kinetics of nucleation and growth during thin-film formation (Ko et al., 2017). Table 2, demonstrated similarly characteristics which indicate a consistent crystalline structure across deposition times, though differences in intensity counts suggest variations in the structural alignment or density of crystallographic planes within the thin film. Also from Figure 3 and Table 4 shows the XRD result of the thin-film deposition at 15 minutes and two notable peaks at 2θ angles degrees of 45.2˚ and 65.4°, with respective intensity counts of 26.61 and 12.69 was obtained. The observed differences in peak intensities for this deposition collaborate the findings of Al-Gaashani et al. (2012)(Dulmaa et al., 2021) who found out that peak intensities in ZnO and CuO nanostructures increased with longer deposition times, suggesting that extended deposition promotes greater crystallinity and alignment within the thin film lattice.

Table 4, also agrees that higher intensity peaks generally correspond to more prominent lattice planes within the crystal structure which aligns with the report by Contreras et al., (2017) that increasing deposition time enhanced the intensity of prominent XRD peaks for metal oxide nanoparticles and samples with longer deposition time tend to exhibit stable crystal sizes and intensities. The peak at 2θ=45.22^{o} ° with an intensity of 26.61 was likely the strongest reflection and which suggested the primary crystalline orientation of the sample. In addition, crystal size calculations using the Scherrer equation show consistent values of approximately 4.65 nm and 5.5 nm, regardless of deposition time. This consistency is significant because it reflects that deposition time variations primarily affect the density and arrangement of lattice planes rather than the crystal size itself. Similar findings were reported by Kumar et al. (2020), who found that in MnO_2 nanoparticle films, peak broadening varied with deposition time but did not significantly alter crystal size due to the limitations imposed by the Scherrer effect on particle size growth. When compared with the control element, Silicon Iron Steel (Table 5), which showed higher intensity peaks (28.43 and 40.06 counts) at the same 2θ values, it can be inferred that $KMnO_4$-deposited films exhibit lower peak intensities, which suggested less crystallinity than Silicon Iron Steel. This difference in crystallinity aligns with the function of $KMnO_4$ in creating a thin film with higher resistivity, which is ideal for reducing eddy current losses as opined by the research of Wu et al., (2019). The lower crystallinity in $KMnO_4$ deposited films reduces the availability of free electrons, thereby reducing conductivity and promoting eddy current loss reduction, a principle that has been well-documented in transformer core research by Wu et al., (2019).

The electrical properties of the thin films, specifically resistivity and conductivity, were investigated to better understand their impact on eddy current losses (Table 6,). Sample X4, which was deposited for 20 minutes, had the highest resistivity (41.04 Ohms/meter) and the lowest conductivity (0.0243 Siemens), indicating a higher resistance to eddy current flow, reducing energy dissipation as heat. An evaluation of Samples X3 (15 minutes deposition) and that of X4 indicates that increasing the deposition time marginally increases resistivity and decreases conductivity. According to the findings of (Al-Bataineh et al., 2022), control sample XE will have the highest eddy current losses since it has the lowest resistivity (37.24 Ohms/meter) and the highest conductivity (0.0268 Siemens). The findings are briefly represented by bar graphs for resistivity (Figure 8) and conductivity (Figure 9). These results underscore that longer deposition times of KMnO4 nanoparticles in thin films increase resistivity and lower conductivity. The greater resistivity inhibits the paths for the formation of eddy currents, effectively reducing eddy current losses and transformer core energy efficiency. Optimizing deposition times, then, may enable the engineering of thin film coatings for transformer cores that will be efficient at reducing energy losses associated with eddy currents. The study focused on comparing nanotechnology enhanced transformers with traditional iron core transformers, specifically evaluating their performance in terms of energy efficiency, resistivity, conductivity, and the reduction of eddy current losses. The comparison is based on the effects of

deposition time which is in line with the study of (Ali et al., 2016) who disclosed that deposition time affect energy loss in transformers. The results show that Potassium Permanganate-enhanced transformers cores exhibit a reduction in eddy current losses due to higher resistivity and lower conductivity, thereby offering greater operational efficiency. Traditional iron core transformers, on the other hand, are more susceptible to higher eddy current losses due to lower resistivity and larger conductivity, resulting in more significant energy dissipation as heat. This comparison further highlights the potential of nanotechnology in significantly improving the energy efficiency of transformers.

CONCLUSION

The study concluded that $KMnO_4$ thin films deposited at a specific observed well well-selected deposition time, can serve as an excellent alternative laminating material for transformer cores. XRD examination confirmed the crystalline nature of the synthesized $KMnO_4$ nanoparticles, with consistent peak positions indicating a stable crystal structure (Figures 2-7, Table 1-5). Furthermore, the films' higher resistivity and lower conductivity, resulting from longer deposition times, effectively mitigate eddy current losses, improving transformer performance and energy efficiency. The findings provide compelling evidence that nanomaterials can improve efficiency by reducing eddy current losses, filling a notable gap in transformer research.

Reference

Al-Bataineh, Q. M., Aljarrah, I. A., Ahmad, A. A., Alsaad, A. M., & Telfah, A. (2022). Investigation of the doping mechanism and electron transition bands of PEO/KMnO4 complex composite films. *Journal of Materials Science: Materials in Electronics*, *33*(17), 14051–14062. https://doi.org/10.1007/s10854-022-08336-0

Ali, A., Zafar, H., Zia, M., ul Haq, I., Phull, A. R., Ali, J. S., & Hussain, A. (2016). Synthesis, characterization, applications, and challenges of iron oxide nanoparticles. *Nanotechnology, Science and Applications*, *Volume 9*, 49–67. https://doi.org/10.2147/nsa.s99986

Arritt, R., & Dugan, R. (2008). Distributed generation interconnection transformer and grounding selection. In *Power and Energy Society General Meeting, IEEE* (pp. 1-6). IEEE. https://doi.org/10.1109/PES.2008.4596772

Cullity, B. D., & Smoluchowski, R. (2014). Elements of X-Ray Diffraction. *Physics Today*, *10*(3), 50–50. https://doi.org/10.1063/1.3060306

Fernández, I., Ortiz, A., Delgado, F., Renedo, C., & Pérez, S. (2013). Comparative evaluation of alternative fluids for power transformers. *Electric Power Systems Research, 98,* 58-69. https://doi.org/10.1016/j.epsr.2012.11.006

Frljić, S., Trkulja, B., & Žiger, I. (2021). Calculation of the eddy current losses in a laminated open-type transformer core based on the A, T−A formulation. *Applied Sciences, 11*(23), 11543. https://doi.org/10.3390/app112311543

Kaur, S., & Kaur, D. (2019). Analysis of effect of core material on the performance of single phase transformer using FEM. *IOP Conference Series: Materials Science and Engineering, 561*(1), 012129. https://doi.org/10.1088/1757899X/561/1/012129

Kumar, S., Islam, T., & Raina, K. K. (2017). Modelling of breather for transformer health assessment. *IET Science, Measurement & Technology, 11*(2), 194-203. https://doi.org/10.1049/iet-smt.2016.0259

Dulmaa, A., Cougnon, F. G., Dedoncker, R., & Depla, D. (2021). On the grain size-thickness correlation for thin films. *Acta Materialia*, *212*, 116896. https://doi.org/10.1016/j.actamat.2021.116896

Ho, M.-Y., Gong, H., Wilk, G. D., Busch, B. W., Green, M. L., Voyles, P. M., Muller, D. A., Bude, M., Lin, W. H., See, A., Loomans, M. E., Lahiri, S. K., & Räisänen, P. I. (2003). Morphology and crystallization kinetics in HfO2 thin films grown by atomic layer deposition. *Journal of Applied Physics*, *93*(3), 1477–1481. https://doi.org/10.1063/1.1534381

Kate, R. S. (2022). *Spray pyrolysis: Approaches for nanostructured metal oxide films in energy storage application*. https://www.academia.edu/105619304/Spray_pyrolysis_Approaches_for_nanostructured_metal_oxide_films_in_energy_storage_application

Ko, H., Sin, D. H., Kim, M., & Cho, K. (2017). Predicting the Morphology of Perovskite Thin Films Produced by Sequential Deposition Method: A Crystal Growth Dynamics Study. *Chemistry of Materials*, *29*(3), 1165–1174. https://doi.org/10.1021/acs.chemmater.6b04507

Olivares-Galván, J. C., Georgilakis, P. S., & Ocon-Valdez, R. (2009). A Review of Transformer Losses. *Electric Power Components and Systems*, *37*(9), 1046–1062. https://doi.org/10.1080/15325000902918990

Ye, Z., Yu, W., Gou, J., Tan, K., Zeng, W., An, B., & Li, Y. (2020). A Calculation Method to Adjust the Short-Circuit Impedance of a Transformer. *IEEE Access*, *8*, 223848–223858. https://doi.org/10.1109/ACCESS.2020.3042983

Patterson, A. L. (2019). Homometric Structures. *Nature*, *143*(3631), 939–940. https://doi.org/10.1038/143939b0

Robertson, J. H. (2012). *Elements of X-ray diffraction* by B. D. Cullity. *Acta Crystallographica Section A*, *35*(2), 350–350. https://doi.org/10.1107/s0567739479000917

Theraja, B. L. (2005). A textbook of electrical technology: Volume I (Basic electrical engineering) (Reprint ed.). S. Chand Publishing.

Wasan R. S., Nada M. S., Wesam A. T., Mohammed A. (2012). Advances in Materials Physics and Chemistry *11*(2).

Wu, X., , Li, H., , Cheng, K., , Qiu, H., , & Yang, J., (2019). Modified graphene/polyimide composite films with strongly enhanced thermal conductivity. *Nanoscale, 11*(17), 8219–8225. https://doi.org/10.1039/c9nr02117e

Ye et al. (2020). *A calculation method to adjust the short-circuit impedance of a transformer*, which discusses short-circuit impedance related to insulation challenges in transformers.

Yu, W., Ye, Z., Gou, J., Tan, K., Cai, J., & Luo, J. (2020). Effects of iron core materials on a single-phase power transformer during out-of-phase synchronisation in MicroGrid. In *2020 IEEE 4th Conference on Energy Internet and Energy System Integration (EI2)* (pp. 1593-1598). IEEE. https://doi.org/10.1109/EI250167.2020.9347065